Journal of Solid State Electrochemistry (2019) 23:1641–1650
https://doi.org/10.1007/s10008-019-04261-1

ORIGINAL PAPER

Quantum conductance investigation on carbon nanotube–based antibiotic sensor

Milad Moutab Sahihazar[1] · Mohammad Taghi Ahmadi[1] · Mina Nouri[1] · Meisam Rahmani[2]

Received: 11 January 2019 / Revised: 17 March 2019 / Accepted: 25 March 2019 / Published online: 11 April 2019

Abstract

Nanostructured carbon material (NSCM) based chemiresistive sensors are popular for sensing different analytes because of their high sensitivity, low cost, and simple construction compared with the conventional sensors. In this paper, the carbon strand (bulk) containing carbon nanostructured materials is fabricated through high-density polyethylene (HDPE). HDPE has been used as a carbon source and carbon strand is grown by pulsed arc discharge method between two hollow metallic rods in the presence of the HDPE. Later on, these electrodes have been used as contacts in the proposed structure. The analyzed structure as a quasi-metallic multi-walled carbon nanotube (MWCNT) based chemiresistive sensor is considered for electrochemical sensing of amoxicillin, penicillin-G, and ampicillin antibiotics. Therefore, the MWCNT quantum conductance as a modeling platform is employed. Finally, current-voltage (*I-V*) characteristics of samples are investigated in the presence of antibiotic materials for different conditions. To this end, the proposed model is compared with experimental data and favorable agreement is reported.

Keywords Quantum conductance · Transmission probability · *I-V* characteristic · Quasi-metallic MWCNT · Chemiresistive sensors · Antibiotic

Introduction

Despite widespread spectrum of antibiotic applications in various fields like human and veterinary medicine for prevention and treatment of infectious diseases, livestock production for growth promotion, agriculture, and aquaculture [1–4], these drugs are one of the main environmental pollutants which entered into aqueous environments by excreting urine and feces through human and animal [5], discharge of hospital wastes, and pharmaceutical company garbage [6]. The emergence of antibiotic-resistant bacterial strains [7], disturbance of normal ecological equilibrium, increase in allergic reaction [8], and entering antibiotics in the human food chain by means of daily food production [8] are problems that their high use rates have serious hazards for the human health and aquatic and soil organisms. Considering all the above-mentioned, the sensing and analysis of antibiotics are a very vital issue in water sources. Chromatographic methods are the most conventional analytical techniques for antibiotic detection with accuracy, but often have some shortages such as real-time detection, equipment of experienced staff, and expensive apparatuses [9, 10]. Commercial test kits are available for the rapid detection of antibiotics; however, these kits have low sensitivity [11]. The optical, colorimetric, electrochemical, and other methods have been commonly employed in the antibiotic detection; however, these techniques possess advantages and disadvantages, and need to study for development of sensitive and portable sensors [12]. Hence, the carbon nanomaterials such as carbon nanotubes (CNTs) have been attracted much attention in fabrication of sensors and biosensors [13] due to high surface area, fast electron transfer rate, thermal and chemical stability, conducting or semiconducting behavior, etc. [14, 15]. In fact, the CNTs play a significant role in the development of ultrasensitive sensors because of hollow tubular geometry that allows binding high rate of target molecules on the CNT surface [16]. Also, a field effect transistor (FET) configuration can make portable sensors. In this configuration, the CNT is used as the conducting channel in the distance between the source and drain electrodes. Gate voltage

✉ Milad Moutab Sahihazar
milad.moutab@yahoo.com

1 Department of Nanotechnology, Urmia University, Urmia, Azerbaijan, Iran

2 Department of Electrical Engineering, Amirkabir University of Technology, 424 Hafez Ave, Tehran, Azerbaijan, Iran

is applied into buffer solution by using Ag/AgCl reference electrode for setting electrostatic potential of solution. Ions are accumulated near the CNT surface and induce opposite charges on the CNT surface; therefore, the CNT channel conductance changes [17]. The conducting channel can be as a CNT or a network of CNTs [18]. This paper focused on the analytical investigation of the antibiotics sensing based on carbon nanoparticle using the *I-V* characteristics. Also, this simplified sensor is composed of classical amperometric and potentiometric sensors. Various analytical methods have been reported for the separation and determination of antibiotics [19–23]. Electrochemical determination of antibiotic sensitivity using carbon ionic liquid electrode by analysis of cyclic voltammetric response has been reported in the literature [19]. Novel electrochemical sensor for the direct determination of pyrazinamide (PZA) using a poly(glycine)-modified glassy carbon electrode (poly(Gly)/GCE) by cyclic and square-wave voltammetry was applied in the reference [20]. The electrochemical determination and oxidation of ceftriaxone were investigated on a GCE-decorated platinum nanoparticle (PtNPs) and carbon nanotube (CNT) [21, 22], in a phosphate buffer solution, and kinetic parameters using cyclic voltammetric studies were extracted [22]. Other analytical applied methods reported for the electrochemical determination of antibiotics in pharmaceutical formulations include capillary electrophoresis, spectroscopic methods, and chemiluminescence [19, 23].

In the presented paper, a carbon strand (bulk) based sensor is fabricated for electrical sensing of three types of beta-lactam antibiotics (amoxicillin, penicillin, and ampicillin). The carbon strand is synthesized by pulsed arc discharge method in the distance between the source and drain electrodes and high-density polyethylene (HDPE) is used as the carbon source. Adsorption of antibiotic molecules on the carbon strand can change its electrical conductance. For rationalizing of antibiotic adsorption mechanism on the carbon strand containing NSCMs, we assume a MWCNT instead of a carbon strand to facilitate achievable modeling. The current-voltage (*I-V*) characteristics of synthesized samples as proposed sensor are investigated before and after sensing process in the different concentrations and temperature values of antibiotic solution. At last, the sensor response is analytically modeled for a sensor based on a MWCNT which shows an acceptable agreement with experimental data. Also, the presented sensor can sense β-lactam antibiotic concentration as low as ppm.

Theory and method

Sensor fabrication and experiment

A sensor is a device that converts physicochemical interaction between target and sensing element to a measurable external signal. The target can change the capacitance, conductance, mass, or other properties of the sensing element [24]. In the work presented, a metallic MWCNT-based chemiresistive sensor is proposed for sensing of three types of beta-lactam antibiotics. Arc discharge technique is one of the nanostructured carbon material (NSCM) producing methods that has been developed [25–28] for using in polyethylene glycol solution as a liquid medium with hollow metallic electrodes. In this work, a high-voltage generator is connected to hollow electrodes mounted in molten HDPE, and this setup is placed on a glassy substrate sheet where the HDPE is heated by a heating system. By this configuration, the NSCM strand grew in the distance between two narrow hollow rods as the conducting channel, as shown in Fig. 1.

Carbon nanostructure strand fabrication is entirely explained as sensor at recent researches [25–28]. Fortunately, in this method, the carbon strand is stably established after cooling of melted HDPE and is connected to electrodes as head-to-head form. Main products of nanomaterial strand are MWCNTs that are randomly localized close to each other and the existence of MWCNTs has been confirmed by analytical techniques in the reference [25]. Using MWCNTs at sensors enhances sensor sensitivity due to their high surface area [29], sensitivity to very small environmental changes [30], and faster electron transfer rate.

In the proposed sensor, hollow rods as metallic electrodes [26] are connected to the drain and source terminals [31] of Autolab probes for measuring of *I-V* curves of carbon strand as shown in Fig. 2. Hence, *I-V* curves of the several synthesized samples are measured as bare sensor before entrance of analyte material.

Combination of pure antibiotic and distilled water as antibiotic solution is injected by hollow rods to carbon strand with different solution concentrations and temperatures, respectively for approaching to modeling steps. The experiment is done on more than 18 samples for any antibiotic and range of overlap on the same quantities indicates device repeatability/reproducibility. The adsorption of antibiotic molecules (target) onto the surfaces of NSCMs strand can change the *I-V* characteristics via electrostatic interactions (charge transfer between the NSCMs and target). Capture content of the target molecules between porous surfaces changes of Schottky barrier height at electrode-MWCNT junctions [32]. Also, length and temperature of carbon strand can be other effective factors on the displacement of *I-V* characteristics. In the next section, the presented model is defined on a MWCNT conductance and contact resistance between the carbon strand and hollow rods is assumed to be small compared to the intrinsic resistance of strand [31].

Proposed model

The aim of this section is to investigate the antibiotic sensing mechanism on a metallic conductor. In the simplified model,

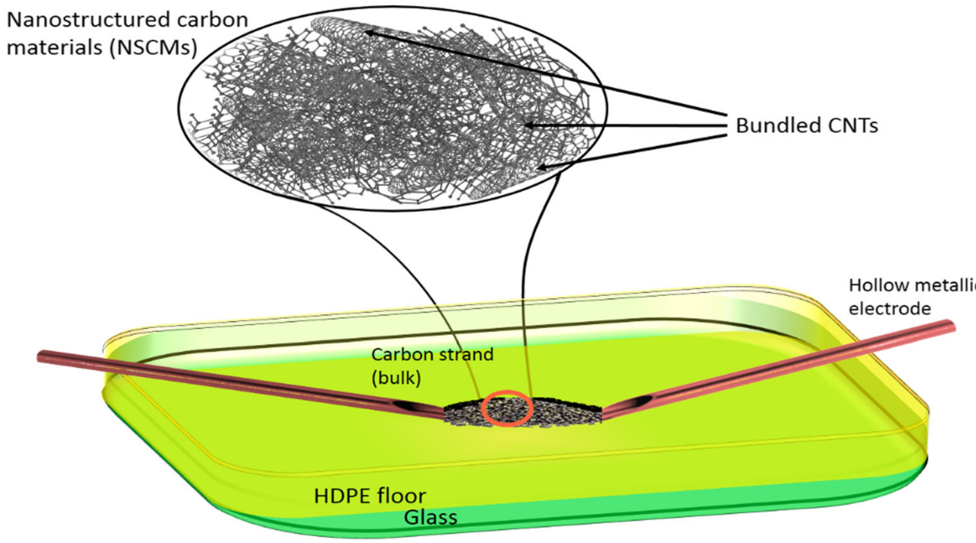

Fig. 1 A schematic diagram of NSCMs grown into the environment of HDPE between two hollow electrodes

electrons can be exited and transported without scattering under non-ballistic conditions [33] in the conductive MWCNT by applying an external potential between two ends of metallic electrodes. In order to elucidate our insight, we will start using MWCNT quantum conductance formula and derive the electrical properties of nanotubes and then employ the bipartite probability of electrons propagating after and before antibiotic injection. MWCNTs are formed of multiple concentric shells d_{shell} of single-walled carbon nanotubes (SWCNTs) with different outer and inner diameters [33]. MWCNTs consisting of more than three shells display metallic characteristics, and even semiconducting shells at room temperature can be quasi-metallic [33]. An ideal state of electron transport in multi-walled nanotube (MWNT) is justified at a one-dimensional (1D) ballistic condition that the strand or nanomaterial dimensions L are much less than mean free path l_{mfp} of electron transport [34, 35]. In addition, nanotubes are connected to reservoirs of electrons; however, reservoir contacts cause identical transparent connections to all shells and electrons can move through the conductor without scattering [33]. Electrical conductance of the MWCNT is a linear sum of the conductance per shell [36]. MWCNTs quantum conductance $G_{q,\ mw}$ can be written as a derivative of the ballistic current and applied drain to source voltage V [33]:

$$G_{q,mw} = \sum_{d_s} \frac{\partial I}{\partial V} = N_{ch} G_0 \qquad (1)$$

After the expansion of above relation and solution of integrals that are related to hole and electron terms, it leads to a general formula $G_{q,\ mw} = N_{ch}G_0$ for the MWNTs quantum conductance with shells of arbitrary chirality, where N_{ch} is

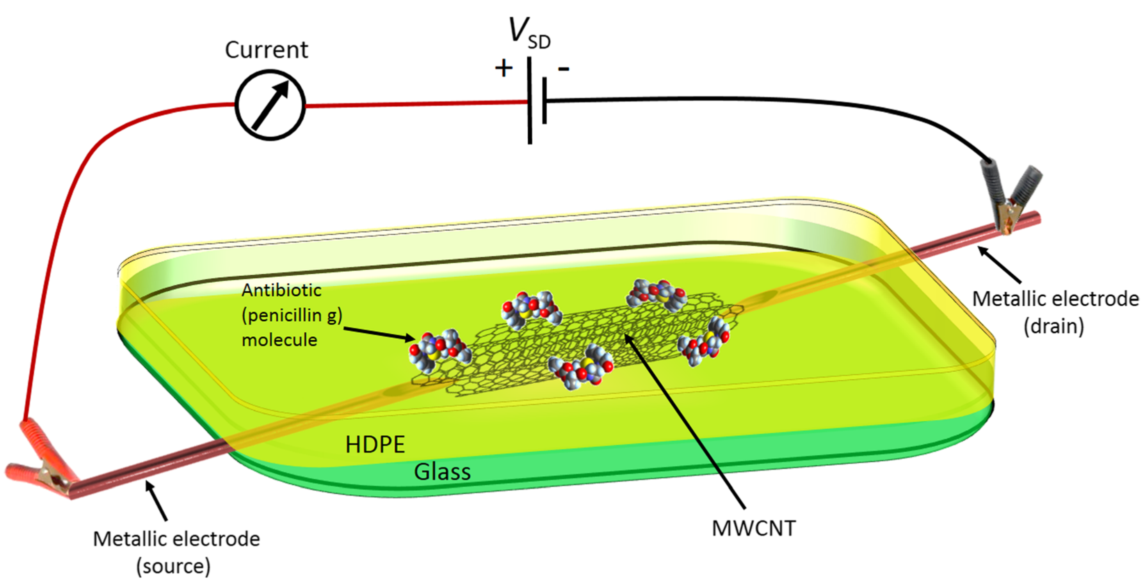

Fig. 2 A schematic diagram of solution injection, penicillin-G adsorption on MWCNT, and measuring of *I-V* characteristics

called total number of propagating channels or modes and $G_0 = \frac{2e^2}{h}$ is a basic constant unit of quantum conductance [37]. Standard average value of the number of MWNT conducting channels is approximately calculated as a function of the nanotube temperature T_{MWNT} and shell diameter d_{shell} with constants a_1 and a_2, under low-bias condition [38]:

$$N_{ch,avg}(d_{shell}, T_{MWNT}) \approx a_1 d_{shell} T_{MWNT} + a_2 \quad (2)$$

Increasing the diameter or temperature linearly increases the number of conduction channels in large shells and also counteracts increasing electron–phonon scattering rate [36, 39]. That is while in small-diameter nanotubes, increasing the temperature or diameter does not change the number of conduction channels [38]. The total number of MWNT channels is a linear sum of the average channels of each shell [33]:

$$N_{ch,avg} = \sum_{d_s} N_{ch,avg}(d_{shell}, T_{MWNT}) \quad (3)$$

Total number of channels in the general form can be achieved by a solution of finite series for a MWNT that depends on the total number of shells, inner-outer diameters, and temperature.

$$N_{ch,avg} = N_{shells}\left(a_1 T_{MWNT}\frac{d_{out}+d_{in}}{2} + a_2\right) \quad (4)$$

Standard statistical random distribution of nanotube chiralities expresses on average 1/3 (metallic shell) + 2/3 (semiconducting shell) for all of the nanotube shells [33]. Generally, transmission of electron on the conductive nanotube is classified into two theories. One is the ballistic theory that electrons can be able to transport in a conductor without any scattering. Another is diffusive theory that experience periodic scattering during transmission through a lattice [33]. A special state nearby ballistic theory, where the device or nanomaterial dimensions and mean free path l_{mfp} establish scattering condition($L \gg l_{mfp}$), general quantum conductance is improved as Landaur's formula [33]:

$$G_{q,mw} = G_0 N_{ch,avg} P \quad (5)$$

where P is considered as a transmission coefficient or probability of electrons propagating without scattering through the strand channels [33]. Also, elastic scattering can be considered for this quantum conductance that affects the transmission coefficients directly and thereby reduces the conductance [40]. Range of propagating probability is elucidated to $0 < P < 1$ and $P = 1$ satisfies ballistic theory [33]. A MWCNT strand is considered as a conductor consisting of two contactive sections in series at the classical transport theory. An electron can transmit directly into both sections and eventually can transmit after the number of reflections [41]. Therefore, general internal transmission probability is represented by deducing of transmission of classical particles as a function of the conductor length L [36]:

$$P_{int} = \gamma \frac{l_{mfp}}{L + l_{mfp}} \quad (6)$$

where γ as a fitting parameter is derived from overlapping of experimental and theoretical *I-V* curves and it has a constant number defined in a certain range that is obtained experimentally from several samples with different lengths, mentioned in Table 1.

The existence of γ coefficient can be caused to the imperfection of MWCNTs replacement, presence of other conductive carbon materials, impurities, and defects in the synthesized carbon strand. The adsorption of antibiotic molecules on the surfaces of carbon strand and their interaction with structural components of strand lead to conversion of its conductance that shown in the form of *I-V* plots. So it can be derived that antibiotic injection to the MWCNT strand affects directly on transmission probability. Therefore, P_{ext} coefficient as an external factor of probability is been entering to general transmission probability as follows (derived from reference [41]):

$$P_{total} = P_{int}.P_{ext} \quad (7)$$

It should be mentioned that P_{ext} is entered into the Landaur's formula in the presence of external factor (antibiotic molecules). In this modeling, we apply the long lengths of MWCNTs equal distance of two electrodes in limits of a few hundred micrometers because long lengths participate at sensible decreasing of conductance in synthesized samples [25, 31]. Checking of two parameters (antibiotic solution concentration and temperature) at experimental linear *I-V* curves after injection of solution is deduced that sensing rate of antibiotic depends on its solution concentration C and temperature$T$. The quantum conductance of MWCNT can be decreased due to exposure and adsorption of ionized molecules by several orders of magnitude [42]. Increasing solution temperature and its equilibrium interaction with carbon strand cause to decreasing of conductance [43] due to shorter lengths of mean free paths [38]. That is while the conductance of short nanotubes increases as temperature rises [38]. These two parameters of antibiotic solution separately affect inversely on the conduction of MWCNT strand $\left(G_{q,mw} \propto \frac{1}{C} \& \frac{1}{T}\right)$. Experimental fitting of two external parameters on the transmission probability assumptively leads to the following formula:

$$P_{ext} = \frac{\alpha}{C} + \frac{\beta}{T} \quad (8)$$

where α and β are constant coefficients, arise from antibiotic solution concentration (ppm) and temperature (K), respectively. Also, they are defined in certain ranges that are obtained experimentally for each type of antibiotic from several

Table 1 Different values and ranges of sample length (L) and fitting parameters (α, β, and γ) respectively corresponding to various conditions for all three types of antibiotics; their average values of modeling are obtained at investigation of several samples

Antibiotic	Different temperatures and concentrations of antibiotic as experimental steps	Range of experimental concentration coefficient in samples (α)	Range of experimental temperature coefficient in samples (β)	Range of applied strand length in the grown samples (L)	Range of fitting constant as internal probability coefficient (γ)	Average coefficients of concentration as modeling parameter ($\alpha_{av.}$)	Average coefficients of temperature as modeling parameter ($\beta_{av.}$)	Average lengths of strands (bulks) at samples modeling ($L_{av.}$)	Average fitting constants as internal probability coefficients ($\gamma_{av.}$)
Penicillin-G	$T_1 = 274$ K, $C = 0.05$ ppm $T_2 = 300$ K, $C = 0.05$ ppm $T_3 = 315$ K, $C = 0.05$ ppm	(28.5–144.4) $\times 10^{-4}$ ppm	(86.81–156) K	(361–455) μm	(264.3–325.7)	86.4×10^{-4} ppm	121.4 K	408 μm	295
	$C_1 = 0.05$ ppm, $T = 300$ K $C_2 = 0.1$ ppm, $T = 300$ K $C_3 = 1$ ppm, $T = 300$ K	(53.2–309.8) $\times 10^{-4}$ ppm	(158.7–232) K	(479–606.2) μm	(205.5–235.9)	181.5×10^{-4} ppm	195.4 K	542.6 μm	220.7
Amoxicillin	$T_1 = 274$ K, $C = 0.05$ ppm $T_2 = 300$ K, $C = 0.05$ ppm $T_3 = 315$ K, $C = 0.05$ ppm	(2.71–6.1) $\times 10^{-4}$ ppm	(160.2–162.4) K	(600–658) μm	(330.9–400.7)	4.4×10^{-4} ppm	161.3 K	629 μm	365.8
	$C_1 = 0.05$ ppm, $T = 300$ K $C_2 = 0.11$ ppm, $T = 300$ K $C_3 = 1$ ppm, $T = 300$ K	(34.8–168) $\times 10^{-4}$ ppm	(214.7–249.4) K	(1097–1186.5) μm	(307.3–346.5)	101.4×10^{-4} ppm	232.1 K	1141.7 μm	326.9
Ampicillin	$T_1 = 274$ K, $C = 0.05$ ppm $T_2 = 300$ K, $C = 0.05$ ppm $T_3 = 315$ K, $C = 0.05$ ppm	(0.6–1.9) $\times 10^{-4}$ ppm	(144.71–145.4) K	(1243–1305.6) μm	(448–654.3)	1.3×10^{-4} ppm	145.1 K	1274.3 μm	551.1
	$C_1 = 0.05$ ppm, $T = 300$ K $C_2 = 0.1$ ppm, $T = 300$ K $C_3 = 1$ ppm, $T = 300$ K	(22.2–132.7) $\times 10^{-4}$ ppm	(106.8–139.2) K	(1004–1286) μm	(328.2–428.4)	77.5×10^{-4} ppm	123 K	1145 μm	378.3

samples of solutions. The purpose of obtaining the transmission probability is to achieve a real fraction number by existing parameters. More effective adsorption parameters were separately considered in the Hamiltonian, overlap, and coupling matrices based on a tight-binding model [44]. Component effects are compared and the effective adsorption parameters are selected in the matrices. Random-matrix approach [45] is separately used for obtaining of composed transmission probability. Approximation effects on applied parameters are investigated and the proposed method presents antibiotic sensing response which helps to detect certain components in the solution. Consequently, matrix effects are taken an amount into account of solved antibiotic sensing by MWCNTs considering of the different experimental aqueous samples. C and T are macroscopic quantities of solution but they are entered into the quantum formula. It can be said that we assume fractions of macroscopic quantities without any unit, in other words, consider existence of effects of antibiotic solution concentration and temperature on quantum conductance. Generally, quantum coherence of synthesized carbon strand as antibiotic sensor and macroscopic solution parameters is interpreted by mesoscopic regime [41, 46] in our proposed method. According to the presented documents and substituting for N_{shells} ($N_{\text{shells}} = 1 + (d_{\text{out}} - d_{\text{in}})/2\delta$) [47], central result of this section is exposed as a closed-form formula:

$$G_{\text{q,mw}} = \sum_{d_s} \frac{\partial I}{\partial V} = G_0\left[\left(1+\frac{d_{\text{out}}-d_{\text{in}}}{2\delta}\right)\left(a_1 T_{\text{MWNT}}\frac{d_{\text{out}}+d_{\text{in}}}{2}+a_2\right)\left(\gamma\frac{l_{\text{mfp}}}{L+l_{\text{mfp}}}\right)\left(\frac{\alpha}{C}+\frac{\beta}{T}\right)\right] \tag{9}$$

It should be mentioned that Eq. (9) is justified for sensing of antibiotic via linear *I-V* curves with solution parameters because of entering of external probability Eq. (8) into the Eq. (9). Also, justification of *I-V* curve in the absence of antibiotic molecules corresponding to a sample fabricated as a bare sensor is yielded without writing of Eq. (8).

Results and discussion

Adsorption and reaction of antibiotic molecules as an external agent with carbon strand affect the slope of the *I-V* characteristics. So, in this regard, Eq. (8) is used which indicates that the transmission probability is composed of two parts (external and internal probability parts). The internal part is related to fundamental and structural properties of strand, so its term (P_{int}) is written in the Eq. (9). But, the second part of probability is considered as the reaction coefficient between antibiotic and carbon molecules. This part can be removed or quantified to a value of 1 (one) in the absence of antibiotic as a bare sensor.

The scrutiny of *I-V* curves demonstrates that the electrical properties of the conductor strand can be justified by quantum conductance of MWCNTs which depends on the number of propagating channels and the conductor length with the fitting parameter γ considering Eqs. 5 and 6. The slope of *I-V* curve is considered as an equation which has been solved in two steps (antibiotic injection and without injection) for obtaining the fitting parameters. Hence, contents of γ are extracted for each similar sample only without antibiotic injection. Penicillin-G solution is injected to several conductive samples at two steps. One of them is done at constant concentration ($C = 0.05$ ppm) of penicillin-G solution and tripartite temperature ($T = 274$, 300, and 315 K), another step at different solution concentrations ($C = 0.05$, 0.1, and 1 ppm) and room temperature of penicillin-G solution. At every step, at first, antibiotic solution is injected to several samples with nearly equal lengths. Ranges of fitting parameters α and β as shown in Table 1 are extracted by resolution of two equations with two unknowns as for slopes of experimental linear *I-V* curves. Injection effectiveness of penicillin-G solution at two practical steps is shown in plots of Fig. 3.

Subsequently, these processes are repeated at various samples with different lengths. Ranges of α and β parameters are individually obtained for each sample. To arrive a comprehensive modeling, checking and comparing of applied lengths of samples and particular ranges of fitting parameters with contents of initial selective sample, all samples can be defined at average ranges of initial sample that are presented in Table 1. It is important that all ranges of obtained contents for sensing of a type of antibiotic are placing in ranges of each other in the employed samples, respectively. The investigation of obtained sample ranges found that every three types of antibiotics materials have a defined proprietary range at each parameter.

The linear *I-V* curves are plotted with details from experimental and modeling data and scrutiny of curves is done. So in this regard, we can justify increasing of conductance with decreasing of penicillin-G solution concentration and temperature. In other words, increasing the solution temperature and its thermodynamic equilibrium with conductor strand causes to increasing of its resistance. Also, existence of penicillin-G molecules and capture of them between porous surfaces and their interaction with context molecules (as bioreceptor) cause to decreasing of electron transmission rate. In *I-V* plots of several samples, overlapping of theoretical modeling on obtained experimental data and identification of a relation between them are associated with a generalized regulation of penicillin-G sensing that is also confirmed for another antibiotics sensing. In this experience, three types of antibiotics (Penicillin-G, Amoxicillin, and Ampicillin) are sensed by carbon conductor strand that is approximately simulated to a MWCNT. Not only is sense modeling obtained for three particular types of antibiotics but also it can be righted for another material. Chemical and physical antibiotic adsorption and also

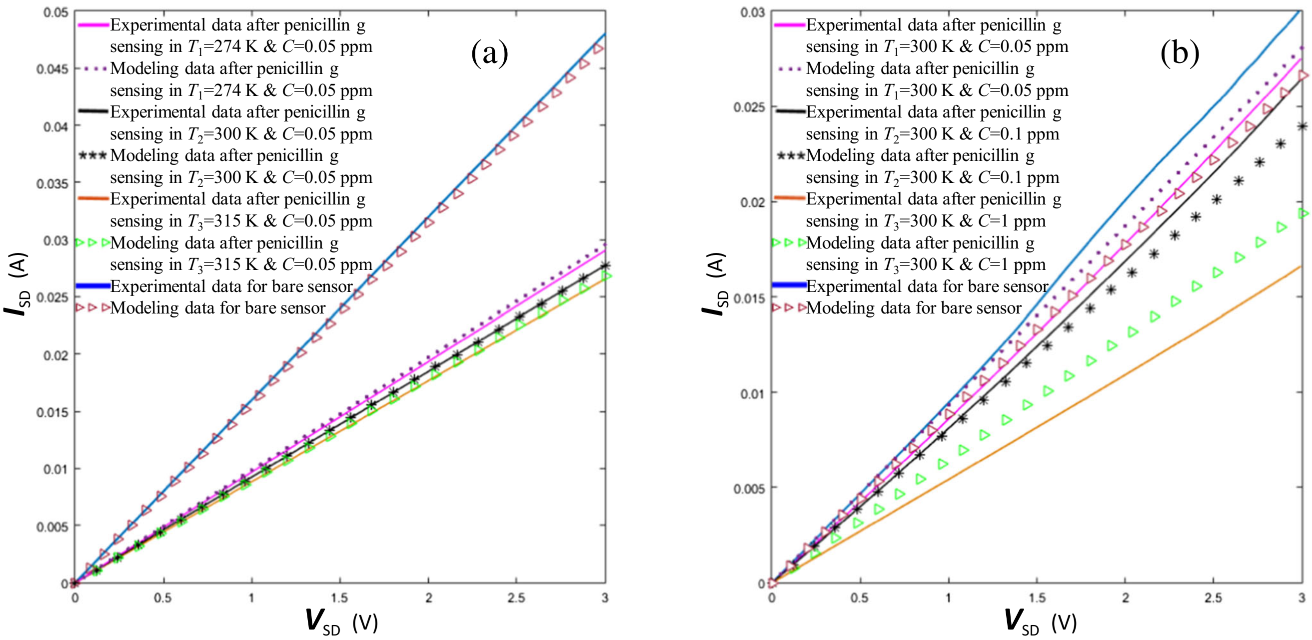

Fig. 3 Comparison of experimental and modeling *I-V* characteristics of penicillin-G sensing by conductive carbon strand at different conditions, **a** C = 0.05 ppm, T = 274, 300, and 315 K and **b** C = 0.05, 0.1, and 1 ppm, T = 300 K

capture of them between porous surfaces (BET surfaces) on carbon strand cause the disturbance of electron transmission. Therefore, *I-V* curves conversion after and before injection is originated from this phenomenon. To get data from Table 1 for the MWCNT conductance modeling, we entered numerical contents of G_0 ($1/G_0 \approx 12.9\ \mathrm{k\Omega}$), for $d_{shell} > 6$ nm, $a_1 \approx 3.87 \times 10^{-4}\ \mathrm{nm^{-1}\ K^{-1}}$, and $a_2 \approx 0.2$ [33, 37]. The mean free path l_{mfp} at low energies in high-quality CNTs is approximately equal to 1 μm at room temperature [31] and the shell-to-shell spacing δ is about the interlayer spacing in graphite ($\delta \sim 0.34$ nm) [33]. It should be noted that the range of d_{out} and d_{in} is in the references [47–50]; the total number of shells N_{shells} is approximately extracted to number 120 [47], and standard average contribution of metallic shells [33] is $N_{shells} = 40$

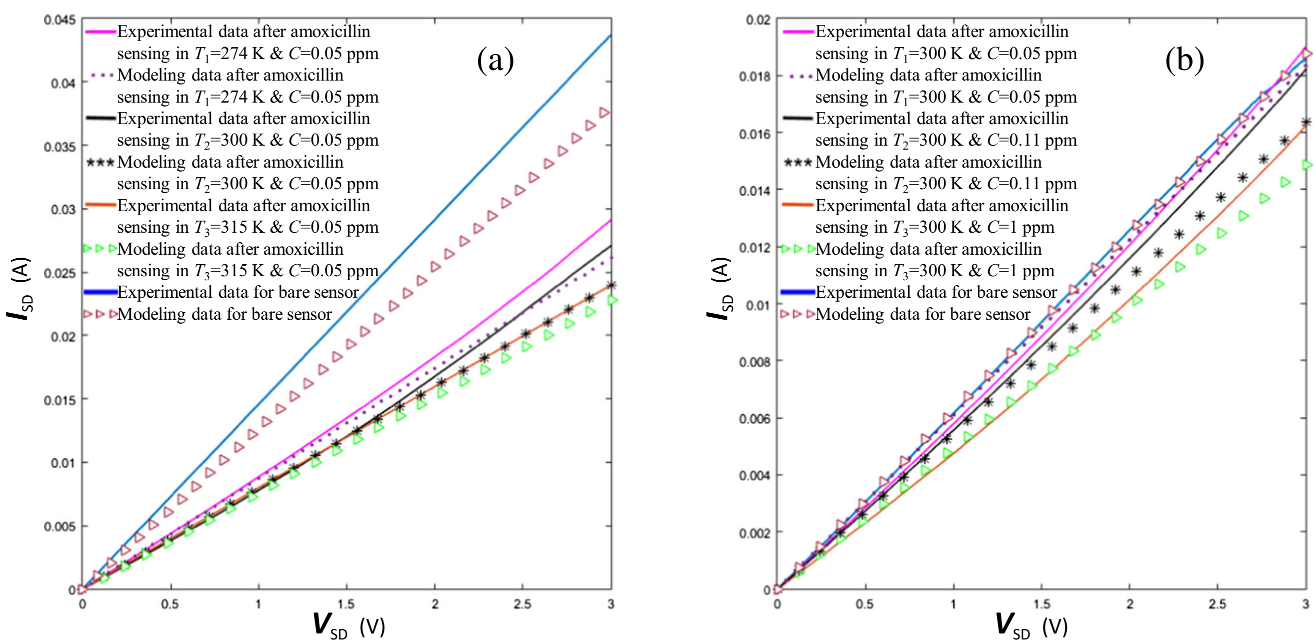

Fig. 4 Comparison of experimental and modeling *I-V* characteristics of amoxicillin sensing by conductive carbon strand at different conditions, **a** C = 0.05 ppm, T = 274, 300, and 315 K and **b** C = 0.05, 0.11, and 1 ppm, T = 300 K

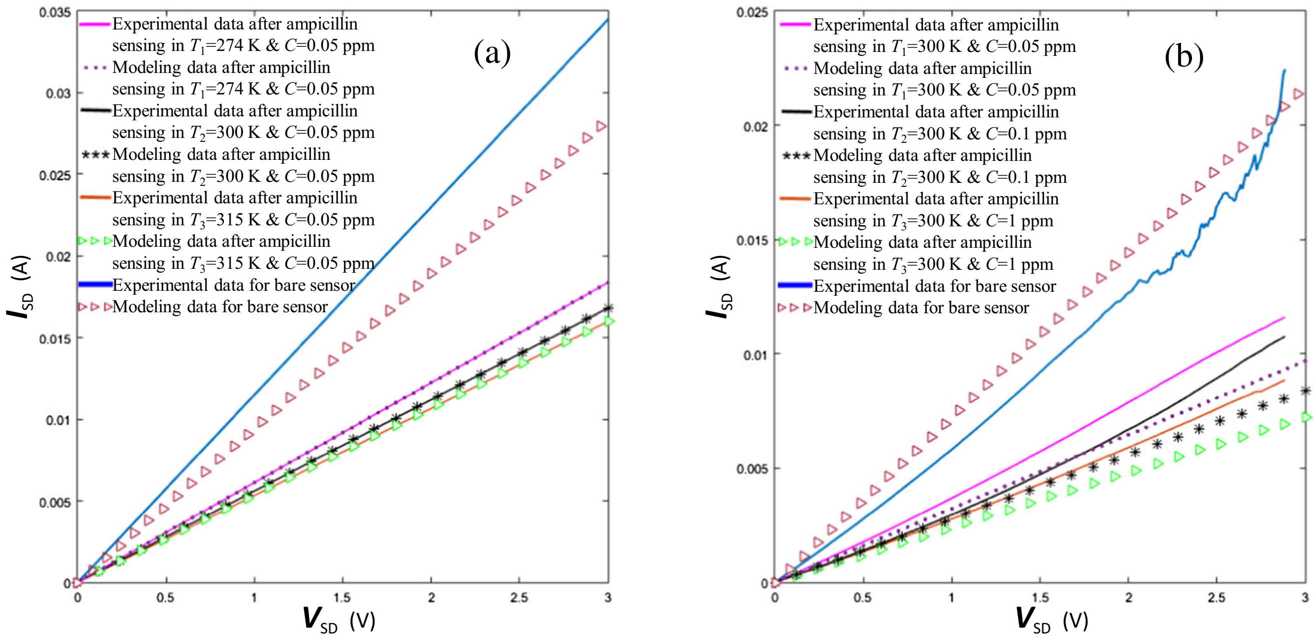

Fig. 5 Comparison of experimental and modeling *I-V* characteristics of ampicillin sensing by conductive carbon strand at different conditions, **a** $C = 0.05$ ppm, $T = 274$, 300, and 315 K and **b** $C = 0.05$, 0.1, and 1 ppm, $T = 300$ K

[47]. The total average number of channels mentioned in Eq. (4) for the MWCNT considered at three different equilibrium temperatures is obtained as $N_{\mathrm{ch,\ avg}} = 282$. Considering of these macroscopic solution parameters (C, T) and their experimental effects on quantum conductance leads us to write an equivalent relation as external probability of antibiotic sensing that is matched with constant fitting parameters expressed in relation (8). It is clear that modeling is originated from electrical conductive properties of carbon strand and every one of antibiotics are sensed with contribution of fitting parameters (α, β, and γ) defined in the certain ranges for any sample. Apart from the three types of antibiotics, we can use other materials with specific fitting parameters obtained experimentally in order to recognize the material type. Adsorption of any antibiotics in the certain temperature and concentration has unique characteristic in the proposed sample. The different samples with different growing conditions have been made and applied for model rationalizing. It is clear that the existence of antibiotic molecules affects electrical conductance of strand. This conversion is observed in other procedures for electrical determination of antibiotic characteristic. It is true that the overlapping of experimental and theoretical *I-V* curves is not entirely done, but the presented model exactly justifies the behavior of their displacing arrangement. Also, investigation and comparison of them with each other are expressed at all three types of antibiotics that *I-V* characteristics are followed from quasi-spectrum logic for the sense conditions as shown in Figs. 3, 4, and 5. These investigations are measured on the approximately equivalent samples that have different structural properties such as distance of two electrodes (strand length), strand growing time, defects, impurities, etc., so according to these reasons, before discriminating and interference studies between the three tested antibiotics must be firstly done in the completely identical grown samples from every aspects.

Conclusion

Carbon strand (bulk) containing MWCNTs plays an important role in the performance of electrochemical sensors due to their remarkable features. In this study, a metallic carbon strand-based chemiresistive sensor is fabricated for electrochemical sensing of three β-lactam antibiotics (Penicillin-G, Amoxicillin, and Ampicillin) successfully. Also, the effect of important parameters such as antibiotic concentration, solution temperature, total number of channels, inner-outer diameter of the MWCNTs, and conductor length are investigated. The quantum conductance as a sensing platform is considered and effective parameters by three constant coefficients (α, β, and γ) are simulated. Finally, comparison study based on *I-V* characteristics is carried out and tolerable agreement between the proposed model and experimental results is reported.

Acknowledgments The authors thank Miss Elnaz Khoramak and Mr. Reza Alizadeh at the Urmia University for their technical support.

References

1. Balarak D, Mostafapour F, Bazrafshan E, Saleh TA (2017) Studies on the adsorption of amoxicillin on multi-wall carbon nanotubes. Water Sci Technol 75:1599–1606

2. Kumar AS, Sornambikai S, Deepika L, Zen J-M (2010) Highly selective immobilization of amoxicillin antibiotic on carbon nanotube modified electrodes and its antibacterial activity. J Mater Chem 20:10152–10158
3. Zervosen A, Sauvage E, Frère J-M, Charlier P, Luxen A (2012) Development of new drugs for an old target—the penicillin binding proteins. Molecules 17:12478–12505
4. Mehrani MJ, Tashayoei MR, Ferdowsi A, Hashemi H (2016) Qualitative evaluation of antibiotics in WWTP and review of some antibiotics removal methods. Int Acad J Sci Eng 3:11–22
5. Ji L, Chen W, Bi J, Zheng S, Xu Z, Zhu D, Alvarez PJ (2010) Adsorption of tetracycline on single-walled and multi-walled carbon nanotubes as affected by aqueous solution chemistry. Environ Toxicol Chem 29:2713–2719
6. Mohammadi A, Kazemipour M, Ranjbar H, Walker RB, Ansari M (2015) Amoxicillin removal from aqueous media using multi-walled carbon nanotubes. Fullerenes, Nanotubes, Carbon Nanostruct 23:165–169
7. Diekema DJ, Pfaller MA (2013) Rapid detection of antibiotic-resistant organism carriage for infection prevention. Clin Infect Dis 56:1614–1620
8. Zhou L, Li D-J, Gai L, Wang J-P, Li Y-B (2012) Electrochemical aptasensor for the detection of tetracycline with multi-walled carbon nanotubes amplification. Sensors Actuators B Chem 162:201–208
9. Yola ML, Eren T, Atar N (2014) Molecularly imprinted electrochemical biosensor based on Fe@ Au nanoparticles involved in 2-aminoethanethiol functionalized multi-walled carbon nanotubes for sensitive determination of cefexime in human plasma. Biosens Bioelectron 60:277–285
10. Moraes FC, Silva TA, Cesarino I, Lanza MR, Machado SA (2013) Antibiotic detection in urine using electrochemical sensors based on vertically aligned carbon nanotubes. Electroanalysis 25:2092–2099
11. Chen B, Ma M, Su X (2010) An amperometric penicillin biosensor with enhanced sensitivity based on co-immobilization of carbon nanotubes, hematein, and β-lactamase on glassy carbon electrode. Anal Chim Acta 674:89–95
12. Lan L, Yao Y, Ping J, Ying Y (2017) Recent advances in nanomaterial-based biosensors for antibiotics detection. Biosens Bioelectron 91:504–514
13. Perez-Lopez B, Merkoci A (2012) Carbon nanotubes and graphene in analytical sciences. Microchim Acta 179:1–16
14. Cesarino I, Moraes FC, Machado SA (2011) A biosensor based on polyaniline-carbon nanotube core-shell for electrochemical detection of pesticides. Electroanalysis 23:2586–2593
15. Kim SN, Rusling JF, Papadimitrakopoulos F (2007) Carbon nanotubes for electronic and electrochemical detection of biomolecules. Adv Mater 19:3214–3228
16. Ramnani P, Saucedo NM, Mulchandani A (2016) Carbon nanomaterial-based electrochemical biosensors for label-free sensing of environmental pollutants. Chemosphere 143:85–98
17. Leyden MR, Schuman C, Sharf T, Kevek J, Remcho VT, Minot ED (2010) Fabrication and characterization of carbon nanotube field-effect transistor biosensors. In: Shinar R, Kymissis I (eds) Organic semiconductors in sensors and bioelectronics III, vol 7779. San Diego, Calif, USA
18. Allen BL, Kichambare PD, Star A (2007) Carbon nanotube field-effect-transistor-based biosensors. Adv Mater 19:1439–1451
19. Absalan G, Akhond M, Ershadifar H (2015) Highly sensitive determination and selective immobilization of amoxicillin using carbon ionic liquid electrode. J Solid State Electrochem 19:2491–2499
20. Ferraz BR, Leite FR, Malagutti AR (2016) Highly sensitive electrocatalytic determination of pyrazinamide using a modified poly (glycine) glassy carbon electrode by square-wave voltammetry. J Solid State Electrochem 20:2509–2516
21. Shahrokhian S, Hosseini-Nassab N, Kamalzadeh Z (2014) Fabrication of an electrochemical sensor based on the electrodeposition of Pt nanoparticles on multiwalled carbon nanotubes film for voltammetric determination of ceftriaxone in the presence of lidocaine, assisted by factorial-based response-surface methodology. J Solid State Electrochem 18:77–88
22. Majdi S, Jabbari A, Heli H, Yadegari H, Moosavi-Movahedi A, Haghgoo S (2009) Electrochemical oxidation and determination of ceftriaxone on a glassy carbon and carbon-nanotube-modified glassy carbon electrodes. J Solid State Electrochem 13:407–416
23. Hasanpour F, Ensafi AA, Khayamian T (2010) Simultaneous chemiluminescence determination of amoxicillin and clavulanic acid using least squares support vector regression. Anal Chim Acta 670:44–50
24. Tang R, Shi Y, Hou Z, Wei L (2017) Carbon nanotube-based chemiresistive sensors. Sensors 17:882
25. Sahihazar MM, Nouri M, Rahmani M, Ahmadi MT, Kasani H (2018) Fabrication of carbon nanoparticle strand under pulsed arc discharge. Plasmonics 13:2377–2386
26. Nouri M, Meshginqalam B, Sahihazar MM, Dizaji RSP, Ahmadi MT, Ismail R (2018) Experimental and theoretical investigation of sensing parameters in carbon nanotube-based DNA sensor. IET Nanobiotechnol 12:1125–1129
27. Kasani H, Khodabakhsh R, Ahmadi MT, Ochbelagh DR, Ismail R (2017) Electrical properties of MWCNT/HDPE composite-based MSM structure under neutron irradiation. J Electron Mater 46: 2548–2555
28. Kasani H, Taghi Ahmadi M, Khoda-Bakhsh R, RezaeiOchbelagh D, Ismail R (2016) Influences of Sr-90 beta-ray irradiation on electrical characteristics of carbon nanoparticles. J Appl Phys 119: 124510
29. Helbling T, Hierold C, Durrer L, Roman C, Pohle R, Fleischer M (2008) Suspended and non-suspended carbon nanotube transistors for NO_2 sensing–a qualitative comparison. Phys Status Solidi B 245:2326–2330
30. Abadi HKF, Ahmadi M, Yusof R, Saeidmanesh M, Rahmani M, Kiani MJ, Ghadiry M (2014) Development of carbon nanotube based biosensors model for detection of single-nucleotide polymorphism. Sci Adv Mater 6:513–519
31. Nshimiyimana JP, Zhang J, Hu X, Chi X, Wu P, Liu S, Zhang Z, Chu W, Sun L (2017) Controlling conducting channels of single-walled carbon nanotube array with atomic force microscopy. Appl Nanosci 7:759–764
32. Wang F, Swager TM (2011) Diverse chemiresistors based upon covalently modified multiwalled carbon nanotubes. J Am Chem Soc 133:11181–11193
33. Wong H-SP, Akinwande D (2011) Carbon nanotube and graphene device physics. Cambridge University Press, Cambridge
34. Imam S-A, Kalam N, Abdhullah S (2014) Temperature dependence of carbon nanotube field effect transistor under non-ballistic conduction considering different dielectric materials. Nanosci Nanotechnol 4:52–58
35. Biercuk MJ, Ilani S, Marcus CM, McEuen PL (2007) Electrical transport in single-wall carbon nanotubes. In: Carbon nanotubes, vol 111. Springer, pp 455-493
36. Naeemi A, Meindl JD (2006) Compact physical models for multiwall carbon-nanotube interconnects. IEEE Electron Device Lett 27: 338–340
37. Naeemi A, Meindl JD (2008) Performance modeling for single-and multiwall carbon nanotubes as signal and power interconnects in gigascale systems. IEEE Trans Electron Devices 55:2574–2582
38. Naeemi A, Meindl JD (2007) Physical modeling of temperature coefficient of resistance for single-and multi-wall carbon nanotube interconnects. IEEE Electron Device Lett 28:135–138
39. Naeemi A, Meindl JD (2005) Impact of electron-phonon scattering on the performance of carbon nanotube interconnects for GSI. IEEE Electron Device Lett 26:476–478

40. Urbina A, Echeverria I, Pérez-Garrido A, Díaz-Sánchez A, Abellán J (2003) Quantum conductance steps in solutions of multiwalled carbon nanotubes. Phys Rev Lett 90:106603
41. Datta S (1997) Electronic transport in mesoscopic systems. Cambridge University Press, Cambridge
42. Bushmaker AW, Oklejas V, Walker D, Hopkins AR, Chen J, Cronin SB (2016) Single-ion adsorption and switching in carbon nanotubes. Nat Commun 7:10475
43. Jarillo-Herrero PD (2005) Quantum transport in carbon nanotubes. Ph.D. thesis, TU Delft, Delft
44. Grujicic M, Cao G, Singh R (2003) The effect of topological defects and oxygen adsorption on the electronic transport properties of single-walled carbon-nanotubes. Appl Surf Sci 211:166–183
45. Takane Y, Wakabayashi K (2003) Random-matrix approach to quantum electron transport in metallic carbon nanotubes. J Phys Soc Jpn 72:2710–2713
46. Das MP (2010) Mesoscopic systems in the quantum realm: fundamental science and applications. Adv Nat Sci Nanosci Nanotechnol 1:043001
47. Close GF, Wong H-SP (2008) Assembly and electrical characterization of multiwall carbon nanotube interconnects. IEEE Trans Nanotechnol 7:596–600
48. Baughman RH, Zakhidov AA, De Heer WA (2002) Carbon nanotubes—the route toward applications. science 297:787–792
49. Li HJ, Lu W, Li J, Bai X, Gu C (2005) Multichannel ballistic transport in multiwall carbon nanotubes. Phys Rev Lett 95:086601
50. Chimowa G, Linganiso EC, Churochkin D, Coville NJ, Bhattacharyya S (2011) Origin of conductivity crossover in entangled multiwalled carbon nanotube networks filled by iron. Phys Rev B 84:205429